Inorganic Chemistry

Article

pubs.acs.org/IC

Synthesis and Structural Characterization of Heterometallic Thorium Aluminum Polynuclear Molecular Clusters

Melissa Fairley, Daniel K. Unruh, Samangi Abeysinghe, and Tori Z. Forbes*

Department of Chemistry, University of Iowa, CB W374, Iowa City, Iowa 52242, United States

Supporting Information

ABSTRACT: Aluminum can undergo hydrolysis in aqueous solutions leading to the formation of soluble molecular clusters, including polynuclear species that range from 1 to 2 nm in diameter. While the behavior of aluminum has been extensively investigated, much less is known about the hydrolysis of more complex mixed-metal systems. This study focuses on the structural characteristics of heterometallic thorium−aluminum molecular species that may have important implications for the speciation of tetravalent actinides in radioactive waste streams and environmental systems. Two mixed metal (Th^{4+}/Al^{3+}) polynuclear species have been synthesized under ambient conditions and structurally characterized by single-crystal X-ray diffraction. $[Th_2Al_6(OH)_{14}(H_2O)_{12}(hedta)_2](NO_3)_6(H_2O)_{12}$ (**ThAl1**) crystallizes in space group $P2_1/c$ with unit cell parameters of a = 11.198(1) Å, b = 14.210(2) Å, c = 23.115(3) Å, and β = 96.375° and $[Th_2Al_8(OH)_{12}(H_2O)_{10}(hdpta)_4](H_2O)_{21}$ (**ThAl2**) was modeled in $P\bar{1}$ with a = 13.136(4) Å, b = 14.481(4) Å, c = 15.819(4) Å, α = 78.480(9)°, β = 65.666(8)°, γ = 78.272(8)°. Infrared spectra were collected on both compounds, confirming complexation of the ligand to the metal center, and thermogravimetric analysis indicated that the thermal degradation of these compounds resulted in the formation of an amorphous product at high temperatures. These mixed metal species have topological relationships to previously characterized aluminum-based polynuclear species and may provide insights into the adsorption of tetravalent actinides on colloidal or mineral surfaces.

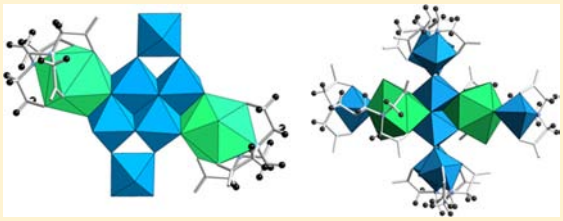

INTRODUCTION

Over the past 50 years, the hydrolysis of aluminum has been extensively investigated because of its importance in industrial processes,[1] wastewater treatment,[2−4] and environmental systems.[5−7] Hydrolysis of aluminum in aqueous solutions is quite complex, encompassing olation reactions, formation of soluble precursors, aggregation, nucleation, and precipitation of solid phases.[8] The speciation of aluminum has been analyzed by potentiometric titrations and NMR spectroscopy, leading to the identification of a variety of species in solution, including monomers, dimers $(Al_2(OH)_2)^{4+}$, trimers $(Al_3(OH)_4)^{5+}$, tridecamers $(Al_{13}O_4(OH)_{24})^{7+}$, and larger polynuclear clusters.[9−12] Under certain conditions, these polynuclear species aggregate to form colloidal or solid amorphous phases and may serve as the fundamental building units of the resulting material.[9] This idea is supported by Furrer et al., 2002, who demonstrated that similar NMR signals are observed for the tridecameric species and amorphous aluminum flocculants.[5]

The structural nature of Al^{3+} polynuclear clusters have been previously investigated and categorized into either "Keggin" or "flat" topologies, with the formation of these different structural forms governed by solution pH and hydrolysis rate.[9,13,14] Keggin-type species are generally observed during titration of an aqueous solution with a base and can be considered a fast hydrolysis scenario.[13,15] These molecules are composed of a central tetrahedrally coordinated AlO_4 group surrounded by 12 additional octahedrally coordinated Al^{3+} cations to create a $[(AlO_4)(Al_{12}(OH)_{24}(H_2O)_{12})]^{7+}$ (Al_{13}) cluster.[13] Five possible isomers exist for the Al_{13} Keggin molecule, although only the ε- and δ-Al_{13} have been observed as isolated species.[16−18] The δ-Al_{13} isomer can also further polymerize to form larger polynuclear clusters (Al_{26}, Al_{30}, and Al_{32}) upon heating or aging of the solution.[18−21] "Flat" molecular species are favored when the synthesis conditions result in slow hydrolysis, such as oxidation of a metal in an acidic solution or in the presence of trapping or chelating ligands.[15,22] These species are built upon cubane-like arrays of octahedrally coordinated Al^{3+} cations linked through bridging hydroxyl groups,[23] and clusters with eight,[24] thirteen,[14,22,25] and fifteen[26] metal centers have been previously synthesized and structurally characterized.

While a basic understanding of the hydrolysis and structural nature of the resulting polynuclear species has been determined for simple solutions, much less is known about more complex mixed-metal systems. Most heterometallic polynuclear species containing Al^{3+} cations include other group 13 metals, such as Ga^{3+} and In^{3+}, or in one case a group 14 cation (Ge^{4+}).[27−30] The central tetrahedrally coordinated Al^{3+} cation in the ε-Al_{13} isomer of the Keggin molecule can be replaced by Ga^{3+} and Ge^{4+} cations, but similar substitutions have not been observed in the δ-Al_{13} isomer or the larger polynuclear species[27,31] Incorporation of d-block metals into aluminum polynuclear species is rare, with only one reported structure that contain octahedrally coordinated W^{6+} substituted into the central

Received: June 19, 2012
Published: August 10, 2012

   dx.doi.org/10.1021/ic3013014 | Inorg. Chem. 2012, 51, 9491−9498

Table 1. Selected Crystallographic Information for ThAl1 and ThAl2

	ThAl1	ThAl2
formula	$[Th_2Al_6(OH)_{14}(H_2O)_{12}(HEDTA)_2](NO_3)_6(H_2O)_{12}$	$[Th_2Al_8(OH)_{12}(H_2O)_{10}(DHPTA)_4](H_2O)_{21}$
FW (g/mol)	2216.68	2710.64
space group	$P2_1/c$	$P\bar{1}$
a (Å)	11.198(1)	13.136(4)
b (Å)	14.210 (2)	14.481(4)
c (Å)	23.115(3)	15.819(4)
α (deg)		78.480(9)
β (deg)	96.375(2)	65.666(8)
γ (deg)		78.272(8)
V (Å^3)	3655.4(7)	2661.8(13)
Z	2	1
ρ_{calc} (g/cm^3)	1.957	1.687
μ (mm^{-3})	4.273	2.976
$F(000)$	2072	1324
crystal size	0.18 mm × 0.16 mm × 0.08 mm	0.11 mm × 0.08 mm × 0.07 mm
θ range (deg)	3.02 to 33.64	2.62 to 25.51
data collected	$-17 < h < 17$	$-15 < h < 15$
	$-22 < k < 22$	$-17 < k < 17$
	$-36 < l < 35$	$-18 < l < 18$
reflections collected/unique	86956/14441 [R_{int} = 0.0320]	57756/9665 [R_{int} = 0.0353]
GOF on F^2	1.101	1.053
final R indices [$I > 2\sigma(I)$]	R_1 = 0.0316, wR_2 = 0.0811	R_1 = 0.0371, wR_2 = 0.1083
R indices (all data)	R_1 = 0.0411, wR_2 = 0.0852	R_1 = 0.0400, wR_2 = 0.1106

region of an Al_{30} cluster.[32] "Flat" Al^{3+} based heterometallic polynuclear species are dominated by molecular clusters with an aluminum core that contains varying amount of a secondary metal, such as In^{3+}, in octahedral coordination. The molecular clusters currently reported in the literature are isostructural to the Al_{13} topology and include the Al_8In_5 and Al_9In_4 clusters.[28,29]

Tetravalent actinides such thorium, uranium, and plutonium readily undergo hydrolysis in aqueous solution, potentially favoring the formation of aluminum-based heterometallic species that may be relevant to a variety of systems.[33] A tetrameric complex containing Fe^{3+} and Th^{4+} cations was recently identified using EXAFS spectroscopy, confirming the existence of heterometallic actinide species in aqueous solutions.[34] These types of molecular species may be important in complex solutions, such as natural aqueous environments, nuclear fuel reprocessing systems, and waste streams. For example, several previous studies have reported that soluble mixed-metal species impact the mobility and bioavailability of tetravalent actinides in surface and subsurface environments, and are enhanced by the presence of organic ligands.[35−37] In addition, heterometallic hydrolysis products may be prevalent in radioactive tank waste at the Hanford site at Hanford, Washington, which contains large amounts of caustic aluminum hydroxide solutions intermixed with a suite of radionuclides.[38,39]

While heterometallic polynuclear clusters containing actinide elements may be present in aqueous solutions, there is limited information on the formation and structural conformation of these species. We have recently begun a series of experiments investigating the structural characteristics of heterometallic molecular clusters based upon aluminum and the early actinide elements that form from aqueous solutions. The current study focuses on the Th^{4+}/Al^{3+} system in the presence of chelating polyaminocarboxylate ligands, hedta (hydroxyethylenediaminetriacetic acid) and hdpta (hydroxyl-1,3-diaminopropane, *N,N,N′,N′*-tetraacetic acid). The addition of chelating ligands, like hedta and hdpta, slows hydrolysis, prevents aggregation and precipitation of colloidal phases, and are potentially relevant for natural aqueous systems, as carboxylate functional groups are prevalent in natural organic matter. Herein, we present the synthesis and characterization of two molecular clusters, $[Th_2Al_6(OH)_{14}(H_2O)_{12}(hedta)_2](NO_3)_6(H_2O)_{12}$ (**ThAl1**) and $[Th_2Al_8(OH)_{12}(H_2O)_{10}(hdpta)_4](H_2O)_{21}$ (**ThAl2**). These compounds represent the first structurally characterized material with mixed Th^{4+}/Al^{3+} metals and offer insights to the hydrolysis products isolated in mixed-metal systems.

EXPERIMENTAL SECTION

Synthesis. **ThAl1** was synthesized by adding 0.350 g of $Al(NO_3)_3{\cdot}9H_2O$ (0.93 mmol) and 0.150 g of $Th(NO_3)_4{\cdot}4H_2O$ (0.27 mmol) to 2.5 mL of deionized water. In a separate vial, 0.62 mmol of the polyaminocarboxylate ligand (0.174 g hedta for **ThAl1** or 0.206 g hdpta for **ThAl2**) was dissolved in 2.5 mL of deionized water. The two solutions were combined, resulting in an overall Th/Al/ligand ratio of approximately 1:3:2, and the pH was adjusted to approximately 5 and 5.8 with pyridine for **ThAl1** and **ThAl2**, respectively. Both samples were allowed to slowly evaporate at room temperature, resulting in the formation of crystals suitable for diffraction studies. Clear blocky crystals of **ThAl1** appeared on the bottom of the vial after approximately four weeks, with overall yields of approximately 5% based upon aluminum content. Crystallization of **ThAl2** was much faster, occurring after approximately one and half weeks with yields of approximately 42%.

Crystallographic Studies. Crystals of **ThAl1** and **ThAl2** were isolated from the mother liquor, coated in Infinium oil to prevent dehydration of the crystals, and mounted on a Nonius Kappa CCD single crystal X-ray diffractometer equipped with MoKα radiation (λ = 0.7107 Å) and a low temperature cryostat. Data collection was performed at 210 K using the Collect software,[40] and unit cell parameters, data integration, and corrections for Lorentzian and polarization parameters were completed using the APEX II suite of software.[41] Absorption corrections were applied using the SADABS program within the APEX II software. Selected data collection parameters and crystallographic information are provided in Table 1.

dx.doi.org/10.1021/ic3013014 | Inorg. Chem. 2012, 51, 9491−9498

ThAl1 and **ThAl2** were solved by direct methods and refined on the basis of F^2 for all unique data using the Bruker SHELXTL version 5.01 software.[42] The Th and Al atoms were found in the direct solution and the O, C, and N atoms were located in the difference Fourier maps calculated following subsequent least-squares refinement of the partial structure models. **ThAl1** crystallizes in monoclinic space group $P2_1/c$ with unit cell parameters of a = 11.198(1) Å, b = 14.210(2) Å, c = 23.115(3) Å, and β = 96.375°. **ThAl2** was originally solved in the triclinic space group $P\bar{1}$, but a center of symmetry was located using the computer program PLATON,[43] resulting in a final structure model with the space group $P1$. The unit cell parameters for **ThAl2** are a = 13.136(4) Å, b = 14.481(4) Å, c = 15.819(4) Å, α = 78.480(9)°, β = 65.666(8)°, γ = 78.272(8)°. Table 2 and 3 list selected bond lengths for **ThAl1** and **ThAl2**, respectively, and crystallographic information files and labeled ball-and-stick models for both compounds are available in the Supporting Information.

Table 2. Selected Bond Distances for ThAl1

Th(1)−O(5)	2.365(2)	Al(2)−O(5)	1.817(2)
Th(1)−O(8)	2.366(2)	Al(2)−O(3)	1.849(2)
Th(1)−O(17)	2.395(2)	Al(2)−O(1)	1.878(2)
Th(1)−O(13)	2.435(2)	Al(2)−O(12)	1.910(2)
Th(1)−O(9)	2.477(2)	Al(2)−O(2)	1.945(2)
Th(1)−O(18)	2.543(2)	Al(2)−O(6)	1.952(2)
Th(1)−O(16)	2.561(3)		
Th(1)−O(6)	2.660(2)	Al(3)−O(4)	1.840(2)
Th(1)−N(1)	2.836(3)	Al(3)−O(1)[a]	1.845(2)
Th(1)−N(2)	2.883(3)	Al(3)−O(11)	1.900(2)
		Al(3)−O(7)	1.905(3)
Al(1)−O(8)	1.825(2)	Al(3)−O(15)	1.928(2)
Al(1)−O(3)[a]	1.848(2)	Al(3)−O(14)	1.933(3)
Al(1)−O(4)	1.850(2)		
Al(1)−O(6)	1.928(2)		
Al(1)−O(2)	1.964(2)		
Al(1)−O(2)[a]	1.966(2)		

[a] $-x, -y + 1, -z$.

Table 3. Selected Bond Distances for ThAl2

Th(1)−O(10)	2.333(3)	Al(2)−O(15)	1.920(4)
Th(1)−O(4)	2.365(3)	Al(2)−O(13)	1.926(4)
Th(1)−O(2)	2.396(4)	Al(2)−O(6)	1.953(4)
Th(1)−O(17)	2.442(4)	Al(2)−N(1)	2.072(5)
Th(1)−O(19)	2.447(4)		
Th(1)−O(3)	2.474(4)	Al(3)−O(8)	1.795(4)
Th(1)−O(14)	2.606(4)	Al(3)−O(11)	1.883(4)
Th(1)−O(1)	2.663(3)	Al(3)−O(7)	1.898(4)
Th(1)−O(22)	2.778(5)	Al(3)−O(15)	1.909(4)
Th(1)−N(3)	2.882(4)	Al(3)−O(12)	1.979(4)
		Al(3)−N(2)	2.081(5)
Al(1)−O(10)	1.872(4)		
Al(1)−O(8)	1.876(4)	Al(4)−O(19)	1.808(4)
Al(1)−O(5)	1.877(4)	Al(4)−O(2)	1.850(4)
Al(1)−O(4)[a]	1.879(4)	Al(4)−O(21)	1.864(6)
Al(1)−O(1)[a]	1.934(4)	Al(4)−O(20)	1.914(6)
Al(1)−O(1)	1.953(4)	Al(4)−O(23)	1.923(6)
		Al(4)−N(4)	2.096(5)
Al(2)−O(5)	1.789(4)		
Al(2)−O(9)	1.885(4)		

[a] $-x, -y + 1, -z + 1$.

Infrared Spectroscopy. The infrared spectra of **ThAl1** and **ThAl2** were collected from 650 to 4000 cm^{-1} using a SensIR technology IlluminatIR FT-IR microspectrometer equipped with a diamond ATR objective. A single crystal was isolated from the mother liquor, placed on a glass slide, and the data was collected in contact mode using a 100 μm aperture.

Thermal Gravimetric Analysis (TGA). The total water content and decomposition temperature of both compounds were determined using a TA Instruments TGA Q500. Approximately 20 mg of each sample was loaded into an aluminum pan and heated in air from 25 to 600 °C at a ramp rate of 2 °C/minute. The samples were cooled to room temperature, and the residual product was characterized by powder X-ray diffraction on a Bruker D5000 instrument (Cu Kα = 1.54 Å) equipped with a LynxEye solid state detector.

RESULTS

Structural Descriptions. The molecular species identified in **ThAl1** contains a core group of six Al^{3+} cations, with two additional Th^{4+} cations located on the outside of the cluster (Figure 1a). Each Al^{3+} cation is octahedrally coordinated by six hydroxyl or water groups with bond lengths ranging from 1.817(2) to 1.966(2) Å. Four of the Al atoms are linked through bridging hydroxyl groups to form an $Al_4(\mu_2\text{-}OH)_{14}(H_2O)_2$ cubane-like moiety that has structural similarities to the sheet topology observed in the mineral brucite ($MgOH_2$). The central aluminum hexamer results from two additional Al polyhedra located on the top and bottom of the molecular cluster that are linked to the tetrameric $Al_4(\mu_2\text{-}OH)_{14}(H_2O)_2$ species in a bridging bidentate fashion. Two Th^{4+} cations are bonded to the aluminum hydroxide core through three hydroxyl groups, resulting in the formation of two shared edges. Each Th^{4+} cation contains additional linkages to the amine, hydroxyl, and carboxylate groups of the hedta molecule and one additional H_2O molecule, resulting in an overall coordination number of ten. Bond distances range from 2.836(3)−2.883(3) Å and 2.365(2)−2.660(2) Å for Th−N and Th−O, respectively. The carboxylate groups of the hedta molecule bonded to the Th atom are deprotonated, but the H atom on the hydroxyl group remains. Overall, the cluster has a Th/Al/hedta ratio of 1:3:1 with a resulting a molecular formula of $[Th_2Al_6(\mu_2\text{-}OH)_{14}(H_2O)_{12}(hedta)_2]^{6+}$.

The molecular species formed in **ThAl1** are quite large, with the longest dimension of the cluster measuring 1.7 nm in length, and are tiled into two-dimensional layers along the [10−2] plane (Figure 1b). The overall charge neutrality of the compound is maintained by the presence of nitrate ions located between the layers. Twelve additional water molecules are also positioned between the clusters and participate in hydrogen bonding with the polynuclear cluster and the oxygen atoms on the nitrate groups with O−H···O distances ranging from 2.62−2.97 Å.

ThAl2 contain a more complex molecular cluster, which can be described by a combination of three distinct dimeric components (Figure 2a). The cluster contains eight Al^{3+} cations, octahedrally coordinated by H_2O, carboxylate, amine, and OH groups, with bond lengths ranging from 1.789(4)−2.096(5) Å. Two Th^{4+} cations present in the cluster are also coordinated by similar functional groups, with a coordination number of ten and bond lengths ranging from 2.096(5)−2.882(4) Å. The central core of the cluster is composed of a $Al_2(OH)_8$ dimer formed through two bridging hydroxyl groups that result in a shared edge. A second aluminum dimer is formed through sharing a single hydroxyl group associated with the hdpta ligand and is further complexed by the four carboxylate groups of the organic chelator. Lastly, a Th/Al dimer is formed in a similar manner with the two metal centers

dx.doi.org/10.1021/ic3013014 | Inorg. Chem. 2012, 51, 9491−9498

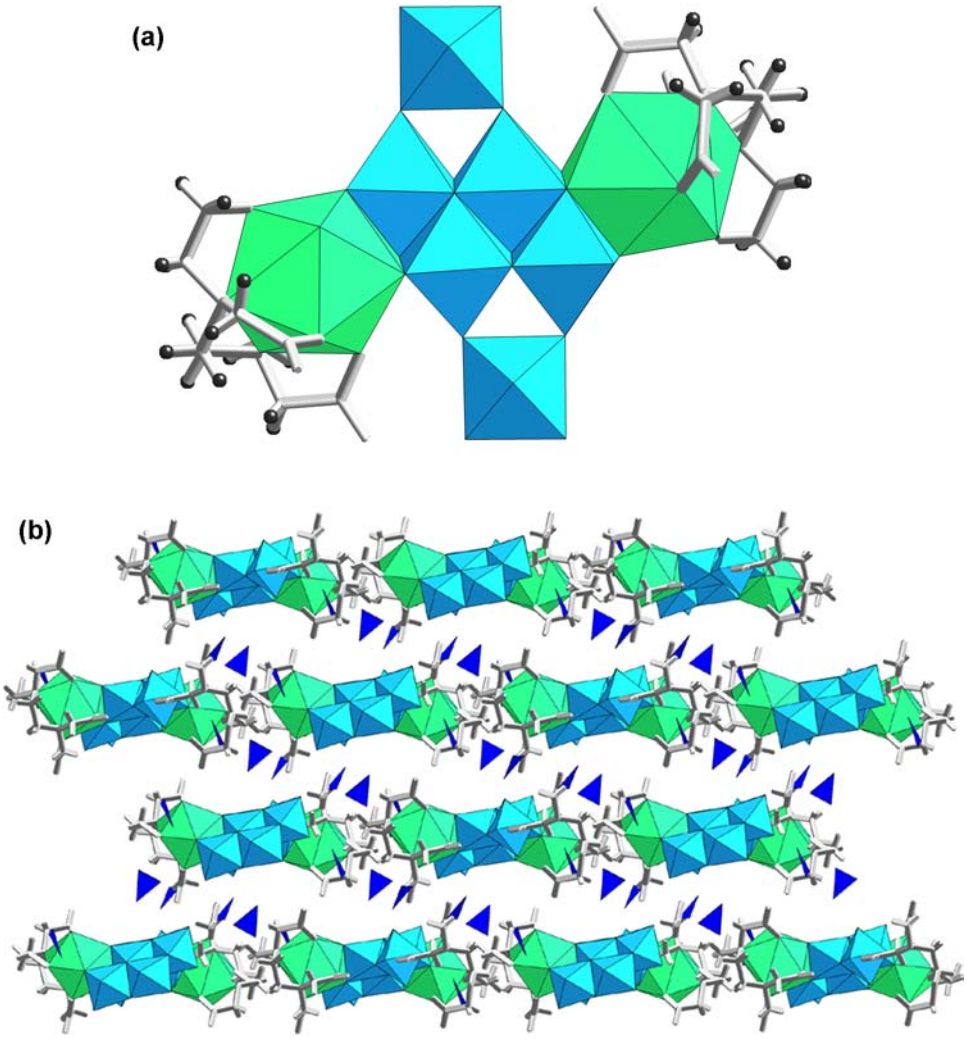

Figure 1. (a) Molecular species observed in **ThAl1** contain six Al atoms (blue polyhedra) bonded to two Th atoms (green polyhedra) that are complexed by the hedta ligand. (b) The Al/Th clusters are tiled into two-dimensional layers and held together by nitrate anions (blue triangles) and H_2O molecules (removed for clarity) in the interlayer.

linked through the deprotonated hydroxyl group on the hdpta molecule.

The dimeric components are then connected into the larger molecular cluster through the formation of additional hydroxyl bridges. The $Al_2(hdpta)(H_2O)_2$ dimers are bonded in a bridging bidentate fashion to the central $Al_2(OH)_8$ dimer, whereas the heterometallic Th/Al dimers are linked to the aluminum core through three bridging hydroxyl groups with the Th^{4+} cation, forming two shared edges. Overall, the cluster has a net neutral charge and a molecular formula of $[Th_2Al_8(OH)_{12}(H_2O)_{10}(hdpta)_4]$. The molecular species measure approximately 1.1 × 1.9 nm and are connected into a three-dimensional lattice through hydrogen bonding with water groups located in the interstitial regions of the cluster (Figure 2b). The O−H···O distances for hydrogen bonding between the interstitial water and the molecular clusters ranges from 2.65 to 2.89 Å.

Infrared Spectroscopy. The spectrum of **ThAl1** is relatively simple, with a broad peak extending from 2567 to 3600 cm^{-1} and two stronger peaks at 1583 and 1335 cm^{-1} (Figure 3a). A broad peak from 3000 to 3600 cm^{-1} and extending to 2567 cm^{-1} indicates the presence of O−H stretching vibrations of the solvent water molecules and hydroxyl stretching vibrations associated with the octahedrally coordinated Al atom.[44] The strong peak at 1583 cm^{-1} most likely corresponds to the asymmetric stretching vibration associated with the −COO group on the hedta molecule. The overall shape of the peak centered at 1335 cm^{-1} in the spectrum suggests the overlap of the symmetric stretching vibrations for the −COO and the N−O stretch of the nitrate groups. The presence of the −COOH functional group would be characterized by a peak at approximately 1700 cm^{-1}, and its absence confirms complexation of the hedta ligand to the metal center.[45] In addition, several weak vibrational modes are present from 820 to 1100 cm^{-1}, corresponding to the carbon backbone of the hedta molecule.

The infrared spectrum of **ThAl2** is much more complex, but contains similarities to vibrational modes present in the **ThAl1** spectrum (Figure 3b). Again, the broad peak extending from 2500 to 3600 cm^{-1} indicates the presence of the interstitial water molecules and octahedrally coordinated aluminum atoms. A water bending mode is located at approximately 1630 cm^{-1} and the slight shift from the expected value of 1640 cm^{-1} suggest that there is additional overlap with the asymmetrical −COO stretching vibration for the hdpta molecule.[45] The strong peak at 1283 cm^{-1} likely corresponds to the symmetric

dx.doi.org/10.1021/ic3013014 | Inorg. Chem. 2012, 51, 9491−9498

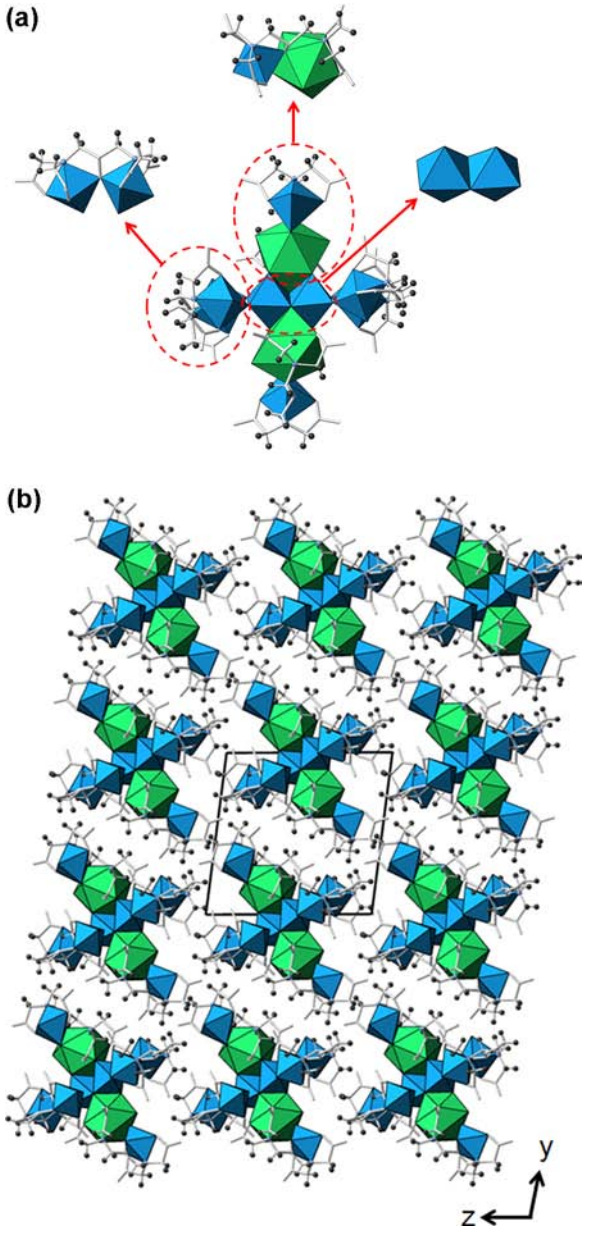

Figure 2. (a) **ThAl2** contains a complex polynuclear cluster that can be described by a combination of several dimeric species, including a central aluminum core, chelated aluminum species, and complexed heterometallic Th/Al unit. (b) The polynuclear species are linked into a three-dimensional lattice through hydrogen bonding with H_2O groups located between the clusters, which have been removed from the figure for clarity.

stretching vibration for deprotonated carboxylate group that is generally observed between 1400 and 1280 cm^{-1} for metal complexes. Weak vibrational modes are again present between 640 and 1150 cm^{-1} and are most likely associated with the aliphatic carbon chain on the hdpta molecule.

Thermal Gravimetric Analysis. Upon heating, **ThAl1** displays a small decrease in mass at approximately 100 °C corresponding to loss of the solvent molecules, followed by decomposition at 220 °C (Figure 4a). Mass loss associated with solvent water molecules was determined to be 10.3% by TGA, which corresponds well to the calculated value of 9.7% for the 12 H_2O molecules identified by single crystal X-ray diffraction. Gradual mass loss continues until 220 °C because of the

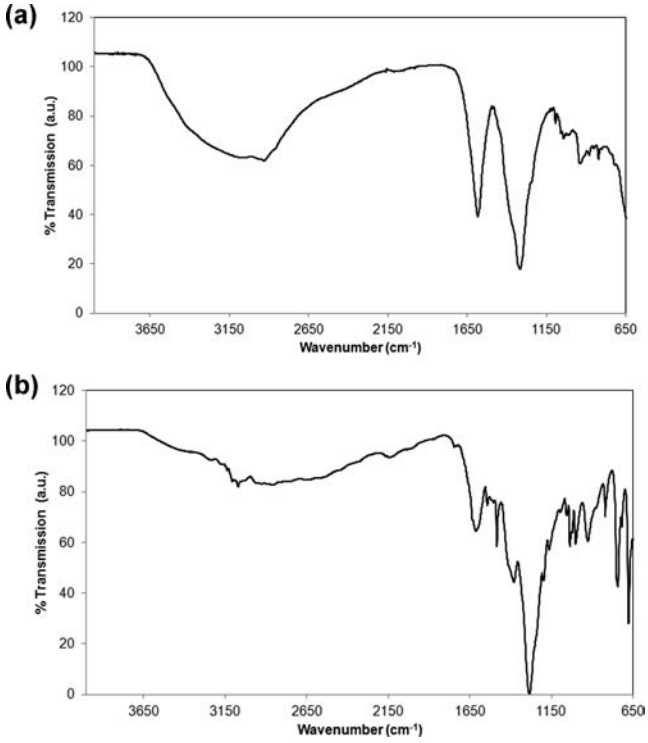

Figure 3. Infrared spectra of (a) **ThAl1** and (b) **ThAl2** indicate the presence of H_2O in the structure and confirm that the carboxylate groups of the organic ligands are complexed to the metal centers of the clusters.

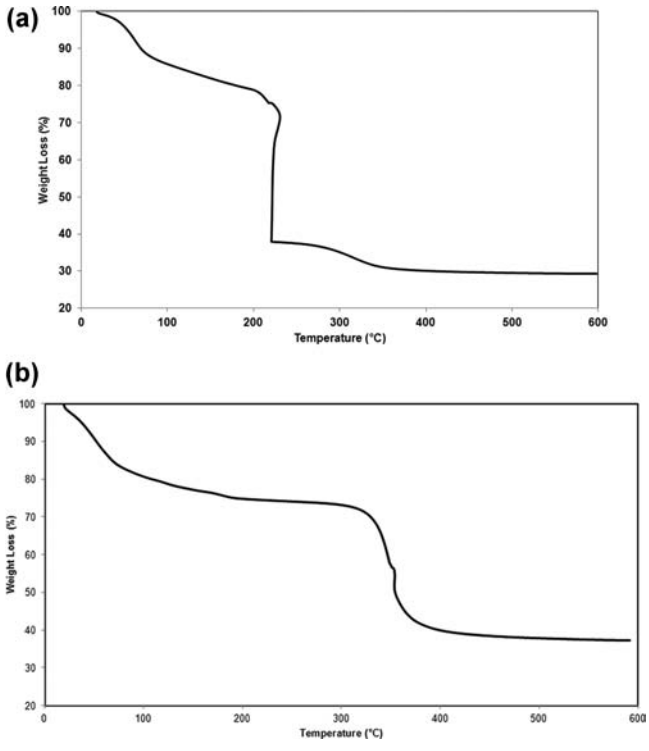

Figure 4. Thermogravimetric analysis of (a) **ThAl1** and (b) **ThAl2** indicate the compounds thermally degrade between 200–400 °C to form an amorphous product.

continued loss of the structural water and hydroxyl groups within the molecular cluster. A decrease of 40.9% occurs at 220 °C and corresponds to the decomposition and loss of both

dx.doi.org/10.1021/ic3013014 | Inorg. Chem. 2012, 51, 9491–9498

hedta ligand and NO_3 from the sample, which is calculated to be 41.5% of the total mass of the compound. The shape of the curve, particularly the slight increase in the temperature during this decomposition suggests that the reaction is relatively exothermic. Additional mass loss after the decomposition of the organic and nitrate constituents is likely due to continued release of structural water. Decomposition of the material is complete at approximately 400 °C resulting in a residual product that is 29.13% of the original mass. The powder X-ray diffraction pattern of the final product after TGA indicates that the material is amorphous, which has also been previously reported for polynuclear aluminum species, as the formation of crystalline γ-alumina generally occurs at higher temperatures (800−1000 °C).[46] The residual mass corresponds relatively well to a mixture of $2ThO_2{\cdot}3Al_2O_3$ or related compound with a calculated value of 27.1%.

The shape of the mass loss curve associated with **ThAl2** is similar to that of **ThAl1**, although breakdown of the hdpta occurs at a slightly higher temperature (Figure 4b). Initial weight loss again corresponds to loss of solvent and structural water, followed by the decomposition of the hpdta ligand at 352 °C. The residual mass of the sample at 600 °C was determined to be 37.2% by TGA that may corresponds to a mixed Th−Al oxide compound and is comparable to a value for the calculated value of 35%. Powder X-ray diffraction confirmed that the final decomposition product formed upon heating **ThAl2** was also amorphous.

DISCUSSION

The polynuclear clusters observed in the **ThAl1** and **ThAl2** compounds are the first structurally characterized heterometallic species formed from hydrolysis of aluminum and thorium in aqueous solutions. While these are the first reported compounds containing aluminum, other heterometallic actinide species can be found in the literature. The incorporation of tetravalent actinides into polytungstophosphate has been of particular focus as these compounds may be used for sequestration and storage of actinides associated with nuclear waste streams.[47,48] Heterometallic clusters containing hexavalent uranium have also been synthesized, including the incorporation of uranium peroxide moieties into a U-shaped P_6W_{36} Wells−Dawson cluster[49] and a mixed U(VI)/Ni(II) cluster containing an ortho-substituted phenylphosphonate to stabilize the cage cluster.[50]

Based upon the structural characteristics of both compounds, **ThAl1** and **ThAl2** can be categorized as "flat" aluminum polynuclear species. The topological features of the core aluminum cluster in **ThAl1** contains similarities to the "flat" $[Al_8(\mu_3\text{-}OH)_2(\mu_2\text{-}OH)_{12}(H_2O)_{18}]^{10+}$ (Al_8) species isolated by Casey et al., 2005.[24] In both molecules, there is a central tetramer composed of four octahedrally coordinated Al^{3+} cations that are further linked to additional Al polyhedra through hydroxyl bridges to form shared vertices. Four additional octahedrally coordinated Al atoms are found at the corners of the tetrameric unit for Al_8, but two are replaced by Th^{4+} cations to create the polymeric species observed in **ThAl1**. The molecular species in **ThAl2** has a unique molecular topology, although several of the structural components have been previously described. The central nonchelated aluminum dimer has been crystallized in a variety of different systems, including those that contain solely inorganic constituents, as well as ones with organic chelating groups, such as nitrilotriacetic acid and iminodiacetic acid.[13,51] Complexation of aluminum by hdpta has not been reported for small dimeric aluminum species, but has been observed in both the Fe(III) and the Cr(III) systems.[52−55] The $[Al_{15}(\mu_3\text{-}O))_4(\mu_3\text{-}OH)_6(\mu_2\text{-}OH)_{14}(hdpta)_4]^{3-}$ (Al_{15}) cluster is also built upon encapsulation of $(Al_7(OH)_{12})^{9+}$ by four dinuclear Al_2(hdpta) units that contains the same coordination geometry as the Al_2(hdpta) units observed in the **ThAl2.**[26]

The coordination geometry of the polyaminocarboxylate ligand to the metal centers differs between the two molecular species, resulting in two very different structural topologies. Presence of the hedta molecule results in chelation of the Th^{4+} cations, whereas the formation of aluminum and mixed-metal dimeric species is favored when the hdpta ligand is added to the solution. The hedta ligand bonds to the Th^{4+} cation through one hydroxyl, two amine, and three carboxylate groups, leaving four additional coordination sites available for bonding to the aluminum polyhedra. A longer carbon chain and presence of an additional hydroxyl group on hdpta creates a different coordination geometry that seems to favors the formation of the dimeric species. The bite angle on the hdpta ligand may not be suitable for encapsulating the Th^{4+}, but more easily accommodates the heterometallic dimeric species, leading to very different structural topologies of the molecular clusters.

Hydrolysis occurs by either the removal of a single proton from a H_2O molecule (olation) or through a two-step mechanism in which an oxo bridge is formed through the release of water as the leaving group (oxolation).[33,56] Hydrolysis of the Al^{3+} cation can take place through either mechanism, although olation is predominant for aquohydroxo complexes and oxolation is only observed in tetrahedral aluminate species.[8] Thorium hydrolysis products identified in solution assume the formation of polynuclear species based upon olation, including dimers ($Th_2(OH)_2^{6+}$, $Th_2(OH)_3^{5+}$, $Th_2(OH)_4^{4+}$), tetramers ($Th_4(OH)_8^{8+}$, $Th_4(OH)_{12}^{4+}$), pentamers ($Th_5(OH)_{12}^{8+}$), and hexamers ($Th_6(OH)_{14}^{10+}$, $Th_6(OH)_{15}^{9+}$).[33,34] Structurally characterized thorium clusters have traditionally been isolated as polynuclear species composed entirely of hydroxo-bridges, but several recent studies have also synthesized mixed hydroxo- and oxo-bridges within the molecular species.[34,57−62]

The interaction of thorium and aluminum in aqueous systems to form heterometallic polynuclear species may be driven by similarities in the hydrolysis mechanism. Bond valence calculations on the O atoms shared between the Th^{4+} and Al^{3+} cations suggest that these are indeed OH groups, indicating that olation is the likely hydrolysis mechanism (Table 4). The preference to form bridging hydroxyl groups for both metal species may lead to more interactions in solution, resulting in the formation of mixed-metal hydrolysis. Further studies are needed to investigate the relationship between hydrolysis mechanism and formation of heterometallic species, as we do acknowledge that the overall product yields were fairly low for both **ThAl1** and **ThAl2.** Crystallization of solid products may not represent all phases present and additional uncharacterized hydrolysis products could remain in the aqueous solution.

Details regarding the hydrolysis of Th^{4+} and Al^{3+} in aqueous solutions and the formation of soluble polynuclear species are currently unavailable, but the related Th^{4+}/Fe^{3+} system has been probed by several techniques. For example, Davydov and Toropov, 1986, observed increase solubility of the Th^{4+}/Fe^{3+} system compared to the related single phases and suggested the formation of heterometallic species in solution.[63] Torapova et

dx.doi.org/10.1021/ic3013014 | Inorg. Chem. 2012, 51, 9491−9498

Table 4. Bond Valence Analysis of the Bridging Hydroxyl Groups between the Th^{4+} and Al^{3+} Cations within the Molecular Clusters Observed in ThAl1 and ThAl2[a]

ThAl1					
	Th1	Al1	Al2	bond valence sum	designation
O5	0.586		0.587	1.173	OH
O6	0.264	0.435		1.106	OH
O8	0.584	0.575		1.159	OH
ThAl2					
	Th1	Al1	Al4	bond valence sum	designation
O1	0.262	0.428		1.118	OH
		0.428			
O2	0.539		0.537	1.076	OH
O4	0.586	0.497		1.082	OH
O10	0.638	0.506		1.145	OH
O19	0.469		0.602	1.071	OH

[a]Bond valence sums and parameters were calculated based upon Brese and O'Keefe, 1991.[69]

al, 2012, corroborated these results with extended X-ray absorption fine structure (EXAFS) spectroscopy and large angle X-ray scattering (LAXS) studies that located a Th_2Fe_2 tetrameric species in solution.[64] Additional potentiometric titrations suggested the formation of polynuclear species with proposed composition of $[Th_2Fe_2(OH)_8(H_2O)_{12}]^{6+}$ and ultrafiltration and X-ray scattering studies indicate that the overall diameter of the cluster is approximately 1.6 nm.[64]

The structural characterization of these two mixed-metal hydrolysis products may also provide insight into the adsorption of actinides onto aluminum colloids and mineral surfaces as Stumm et al., 1987, noted that the ability to interact with surface hydroxyl groups is related to the formation of hydroxo complexes in solution.[65] This relationship was also highlighted by hydrolytic scavenging mechanisms in marine environments, that is, removal of trace elements, such as Th^{4+}, from the water column by fine particles. Whitfield and Turner, 1987, found that that scavenging of trace elements could be correlated to a specific group of elements on a complex field diagram for a seawater system.[66] The complex field diagram groups specific elements into four categories: (A) weakly complexed elements; (B) elements dominated by chloride complexes; (C) strongly hydrolyzed elements; and (D) fully hydrolyzed elements. Hydrolytic scavenging corresponded to the group C (strongly hydrolyzed elements) that contain Al^{3+}, Be^{2+}, Cr^{3+}, Fe^{3+}, Ga^{3+}, Hf^{4+}, Th^{4+}, U^{4+}, and Zr^{4+} cations, linking the adsorption of these elements onto colloidal surfaces to hydrolysis in solution.[66]

Details regarding the structural nature of Th^{4+} adsorption onto the surface of aluminum minerals are unavailable, but the sorption of Th^{4+} onto ferrihydrite has been investigated using EXAFS spectroscopy.[67] The interatomic Th−Fe distances for Th^{4+} adsorbed to the surface of ferrihydrite is 3.56−3.59 Å, which was interpreted as a bidentate corner-sharing configuration with two FeO_6 octahedra located on the mineral surface. As the differences in the ionic radii for Fe^{3+} and Al^{3+} are approximately 0.02 Å, the interatomic distance to the Th^{4+} cation should be similar between the two metals.[68] Bonding between the Th^{4+} and Al^{3+} cations in **ThAl1** and **ThAl2** is identical, forming two shared edges via three hydroxyl bridges and Th−Al distances of 3.552−3.593 Å. The proposed coordination mode for Th^{4+} on the surface of ferrihydrite could easily be converted into two shared edges through an additional bond between the bridging hydroxo/oxo group that connects the FeO_6 octahedra.[67] As little structural evidence is available for the bonding that occurs between Th^{4+} and Al^{3+} or Fe^{3+} polyhedra, the configuration observed in **ThAl1** and **ThAl2** could serve as a starting point in the interpretation of spectroscopic data regarding adsorption onto mineral surfaces.

CONCLUSIONS

The formation of heterometallic polynuclear species may have important implications on the speciation and solubility of tetravalent actinides in aqueous solution, and the structural characterization of **ThAl1** and **ThAl2** offers some insight into the interaction of these components in aqueous solutions. The topological differences between these two compounds suggest that the nature of the organic chelating ligand may influence some of the structural characteristics of the resulting molecular species. Therefore, further structural characterization of species with various polyaminocarboxylates is needed to investigate trends in chelation and similarities in topological features. In addition, the relationship between these polynuclear hydrolysis species and colloidal materials must be more concretely established to provide additional molecular level insight into the transport of actinides in environmental systems.

ASSOCIATED CONTENT

Supporting Information

Crystallographic information in CIF format. Further details are given in Figures S1 and S2. This material is available free of charge via the Internet at http://pubs.acs.org.

AUTHOR INFORMATION

Corresponding Author

*E-mail: tori-forbes@uiowa.edu.

Notes

The authors declare no competing financial interest.

ACKNOWLEDGMENTS

This work was supported by the University of Iowa Vice President of Research Mathematics and Physical Science Program and the University of Iowa College of Liberal Arts and Sciences. We also thank Professor Peter C. Burns at the University of Notre Dame for use of the SensIR technology instrument.

REFERENCES

(1) Trueba, M.; Trasatti, S. P. *Euro. J. .Inorg. Chem.* **2005**, 3393−3403.

(2) Xiaoying, M.; Guangming, Z.; Chang, Z.; Zisong, W.; Jian, Y.; Jianbing, L.; Guohe, H.; Hongliang, L. *J. Colloid Interface Sci.* **2009**, *337*, 408−413.

(3) Chen, Z.; Fan, B.; Peng, X.; Zhang, Z.; Fan, J.; Luan, Z. *Chemosphere* **2006**, *64*, 912−918.

(4) Mertens, J.; Casentini, B.; Masion, A.; Pothig, R.; Wehrli, B.; Furrer, G. *Water Res.* **2012**, *46*, 53−62.

(5) Furrer, G.; Phillips, B. L.; Ulrich, K. U.; Pothig, R.; Casey, W. H. *Science* **2002**, *297*, 2245−2247.

(6) Kawano, M.; Tomita, K. *Clays Clay Miner.* **1996**, *44*, 672−676.

(7) Jones, B. E. H.; Haynes, R. J. *Crit. Rev. Environ. Sci. Technol.* **2011**, *41*, 271−315.

(8) Jolivet, J.-P.; Chaneac, C.; Chiche, D.; Cassaignon, S.; Durupthy, O.; Hernandez, J. C. *R. Geosci.* **2011**, *343*, 113−122.

(9) Fu, G.; Nazar, L. F.; Bain, A. D. *Chem. Mater.* **1991**, *3*, 602−610.

(10) Akitt, J. W.; Elders, J. M. *J. Chem. Soc., Faraday Trans.* **1985**, *81*, 1923−1930.
(11) Akitt, J. W.; Elders, J. M. *J. Chem. Soc., Dalton Trans.* **1988**, 1347−1355.
(12) Akitt, J. W.; Farthing, A. *J. Chem. Soc., Dalton Trans.* **1981**, 1624−1628.
(13) Casey, W. H. *Chem. Rev.* **2006**, *105*, 1−16.
(14) Gatlin, J. T.; Mensinger, Z. L.; Zakharov, L. N.; Macinnes, D.; Johnson, D. W. *Inorg. Chem.* **2008**, *47*, 1267−1269.
(15) Wang, W.; Wentz, K. M.; Hayes, S. E.; Johnson, D. W.; Keszler, D. A. *Inorg. Chem.* **2011**, *50*, 4683−4685.
(16) Johansson, G. *Acta Chem. Scand.* **1960**, *14*, 771−773.
(17) Johansson, G.; Lundgren, G.; Sillen, L. G.; Soderquist, R. *Acta Chem. Scand.* **1960**, *14*, 769−771.
(18) Rowsell, J.; Nazar, L. F. *J. Am. Chem. Soc.* **2000**, 122.
(19) Allouche, L.; Gerardin, C.; Loiseau, T.; Ferey, G.; Taulelle, F. *Angew. Chem., Int. Ed.* **2000**, *39*, 511−514.
(20) Sun, Z.; Wang, H.; Tong, H.; Sun, S. *Inorg. Chem.* **2011**, *50*, 559−564.
(21) Abeysinghe, S.; Unruh, D. K.; Forbes, T. Z. *Cryst. Growth Des.* **2012**, *12*, 2044−2051.
(22) Heath, S. L.; Jordan, P. A.; Johnson, I. D.; Moore, G. R.; Powell, A. K.; Helliwell, M. *J. Inorg. Biochem.* **1995**, *59*, 785−794.
(23) Casey, W. H.; Swaddle, T. W. *Rev. Geophys.* **2003**, *41*, 1−20.
(24) Casey, W. H.; Olmested, M. M.; Phillips, B. L. *Inorg. Chem.* **2005**, *44*, 4888−4890.
(25) Seichter, W.; Mogel, H.-J.; Brand, P.; Salah, D. *Eur. J. Inorg. Chem.* **1998**, 795−797.
(26) Schmitt, W.; Baissa, E.; Mandel, A.; Anson, C. E.; Powell, A. K. *Angew. Chem., Int. Ed.* **2001**, *40*, 3578−3580.
(27) Lee, A. P.; Phillips, B. L.; Olmstead, M. M.; Casey, W. H. *Inorg. Chem.* **2001**, *40*, 4485−4488.
(28) Mensinger, Z. L.; Gatlin, J. T.; Meyers, S. T.; Zakharov, L. N.; Keszler, D. A.; Johnson, D. W. *Angew. Chem., Int. Ed.* **2008**, *47*, 9484−9486.
(29) Mensinger, Z. L.; Wang, W.; Keszler, D. A.; Johnson, D. W. *Chem. Soc. Rev.* **2012**, *41*, 1019−1030.
(30) Bradley, S. M.; Kydd, R. A.; Yamdagni, R. *J. Chem. Soc., Dalton Trans.* **1990**, 2653−2656.
(31) Parker, W. O.; Millini, R.; Kiricsi, I. *Inorg. Chem.* **1997**, *36*, 571−575.
(32) Son, J. H.; Kwon, Y.-U. *Inorg. Chem.* **2003**, *2003*, 4153−4159.
(33) Baes, C. F.; Mesmer, R. E. *The hydrolysis of cations*; John Wiley and Sons: New York, 1976.
(34) Torapava, N.; Persson, I.; Eriksson, L.; Lundberg, D. *Inorg. Chem.* **2009**, *48*, 11712−11723.
(35) Righetto, L.; Bigodlio, G.; Azimonti, G.; Bellobono, I. R. *Environ. Sci. Technol.* **1991**, *25*, 1913−1919.
(36) Moulin, V.; Tits, J.; Ouzounian, G. *Radiochim. Acta* **1992**, *58/69*, 179−190.
(37) Mincher, B. J.; Fox, R. V.; Cooper, D. C.; Groenewold, G. S. *Radiochim. Acta* **2003**, *91*, 397−401.
(38) Wan, J.; Tokunaga, T. K.; Saiz, E.; Larsen, J. T.; Zheng, Z.; Couture, R. A. *Environ. Sci. Technol.* **2004**, *38*, 6066−6073.
(39) Shafer, J. C.; Sulakova, J.; Ogden, M. D.; Nash, K. L. *IOP Conf. Series: Mater. Sci. Eng.* **2010**, *9*, 1−8.
(40) Hoft, R. W. W., Ed.; *Collect*; Nonius, B.V.: Delft, The Netherlands, 1998.
(41) Sheldrick, G. M. *Acta Crystallogr., Sect. A.* **2008**, 64−66.
(42) Sheldrick, G. M. *SHELTXTL*, version 5.01; Bruker AXS: Madison, WI, 1996.
(43) Spek, A. L. *PLATON*; Utrecht University: Utrecht, The Netherlands, 2005.
(44) Teagarden, D. L.; Hem, S. L.; White, J. L. *J. Soc. Cosm. Chem.* **1982**, *33*, 281−295.
(45) Mehrota, R. C.; Bohra, R. *Metal carboxylates*; Academic Press: London, U.K., 1983.
(46) Kloprogge, J. T.; Gueus, J. W.; Jansen, J. B. H.; Seykens, D. *Thermochim. Acta* **1992**, *209*, 265.
(47) Sokolava, M. N.; Fedosseev, A. M.; Andreev, G. B.; Budantseva, N. A.; Yusov, A. B.; Moisy, P. *Inorg. Chem.* **2009**, *48*, 9185−9190.
(48) Chiang, M.-H.; Soderholm, L.; Antonio, M. R. *Eur. J. Inorg. Chem.* **2003**, 2929−2936.
(49) Sankar, S.; Dickman, M. H.; Kortz, U. *Chem.—Eur. J.* **2008**, *14*, 9851−9855.
(50) Adelani, P. O.; Oliver, A. G.; Albrecht-Schmitt, T. E. *Inorg. Chem.* **2012**, *51*, 4885−4887.
(51) Casey, W. H.; Phillips, B. L.; Furrer, G. *Rev. Miner. Geochem.* **2001**, *44*, 167−190.
(52) Schmitt, W.; Anson, C. E.; Pilawa, B.; Powell, A. K. *Z. Anorg. Allg. Chem.* **2002**, *628*, 2443−2457.
(53) Schmitt, W.; Anson, C. E.; Wernsdorfer, W.; Powell, A. K. *Chem. Commun.* **2005**, 2098−2100.
(54) Schmitt, W.; Zhang, L.; Anson, C. E.; Powell, A. K. *Dalton Trans.* **2010**, *39*, 10279−10285.
(55) Mukkamala, S. B.; Clerac, R.; Anson, C. E.; Powell, A. K. *Polyhedron* **2006**, *25*, 530−538.
(56) Henry, M.; Jolivet, J.-P.; Livage, J. *Struct. Bonding (Berlin)* **1992**, *77*, 153−206.
(57) Knope, K. E.; Wilson, R. E.; Vasiliu, M.; Dixon, D. A.; Soderholm, L. *Inorg. Chem.* **2011**, *50*, 9696−9704.
(58) Knope, K. E.; Vasiliu, M.; Dixon, D. A.; Soderholm, L. *Inorg. Chem.* **2012**, *51*, 4239−4249.
(59) Johansson, G. *Acta Chem. Scand.* **1968**, *22*, 399−403.
(60) Kadish, K. M.; Liu, Y. H.; Anderson, J. E.; Charpin, P.; Chevrier, G.; Lance, M.; Nierlich, M.; Vigner, D.; Dormond, A.; Belkalem, B.; Guilard, R. *J. Am. Chem. Soc.* **1988**, *110*, 6455−6462.
(61) Harrowfield, J. M.; Ogden, M. I.; White, A. H. *J. Chem. Soc., Dalton Trans.* **1991**, 2625−2632.
(62) Takao, S.; Takao, K.; Kraus, W.; Ernmerling, F.; Scheinost, A. C.; Bernhard, G.; Hennig, C. *Eur. J. Inorg. Chem.* **2009**, 4771−4775.
(63) Davydov, Y. P.; Toropov, I. G. *Proc. Acad. Sci. Belarus, Chem. Serv.* **1986**, *5*, 7−10.
(64) Torapava, N.; Radkevich, A.; Persson, I.; Davydov, D.; Eriksson, L. *Dalton Trans.* **2012**, *41*, 4451−4459.
(65) Stumm, W.; Wehrli, B.; Wieland, E. *Croatica Chem. Acta* **1987**, *60*, 429−456.
(66) Whitfiled, M.; Turner, D. R. In *Aquatic Surface Chemistry: Chemical processses at the particle-water interface*; Stumm, W., Ed.; John Wiley and Sons: New York, 1987, pp 475−493.
(67) Seco, F.; Hennig, C.; De Pablo, J.; Rovira, M.; Rojo, I.; Marti, V.; Gimenez, J.; Duro, L.; Grive, M.; Bruno. *J. Environ. Sci. Technol.* **2009**, *43*, 2825−2830.
(68) Shannon, R. *Acta Crystallogr.* **1976**, *A32*, 751−767.
(69) Brese, N. E.; O'Keefe, M. *Acta Crystallogr.* **1991**, *B47*, 192−197.